

# Metal Atom Vibrational Amplitudes in Decamethylferrocene and Related Organometallics

Rolfe H. Herber,<sup>\*[a]</sup> Israel Nowik,<sup>[a]</sup> Volker Kahlenberg,<sup>[b]</sup> Holger Kopacka,<sup>[c]</sup> and Herwig Schottenberger<sup>[c]</sup>

**Keywords:** Sandwich complexes / Iron / Vibrational amplitudes / Mössbauer spectroscopy / Isotopic enrichment

Recent experiments have shown that root-mean-square amplitudes-of-vibration (rmsav) for iron atoms in organometallic complexes at various temperatures can be extracted from temperature-dependent  $^{57}\text{Fe}$  Mössbauer spectroscopic data related to the recoil-free fraction of the metal atom. The applicability of this procedure has been validated by comparison with rmsav data extracted from  $U_{ij}$  values obtained from single-crystal X-ray diffraction parameters at various temperatures. This analysis has been applied in detail to a study

of decamethylferrocene (DMFc), for which the agreement between the rmsav values derived from the two experimental procedures is compared in the present study. A comparison of these rmsav values for a number of related structures is also reported over a similar temperature range. An improved method for the quantitative preparation of isotopically enriched DMFc is described.

(© Wiley-VCH Verlag GmbH & Co. KGaA, 69451 Weinheim, Germany, 2006)

## Introduction

In a number of recent publications from this laboratory (HU),<sup>[1–4]</sup> it has been shown that temperature-dependent  $^{57}\text{Fe}$  Mössbauer effect spectroscopy (ME) can serve to elucidate the root-mean-square-amplitude-of-vibration (rmsav) of the metal atom in ferrocene-type organometallics. While such studies have led to reasonably self-consistent values for this parameter, detailed validation has only been accomplished in the case of the parent ferrocene, for which single-crystal X-ray data are available at a number of different temperatures. However, in the case of ferrocene, not only are the details of the molecular structure and arrangement complicated by the existence of a number of different crystallographic forms, but the particular crystallographic form assumed at a given temperature depends on the thermal history of the sample.<sup>[5]</sup> References to these reported X-ray data have been reported earlier.<sup>[4]</sup>

To place the inference concerning the iron atom rmsav in iron organometallics on a more reliable basis, in the present study both the X-ray structure and the detailed ME parameters of decamethylferrocene (DMFc) have been determined at a number of different temperatures, thus allowing a comparison of the values obtained by the two techniques.

There have been a number of X-ray studies of DMFc reported in the literature, but the early work of Struchkov et al.<sup>[6]</sup> has been re-examined by Raymond et al.<sup>[7]</sup> and in neither case are the thermal parameters of the metal atom extractable from the available data. In the present study, single-crystal X-ray diffraction data for DMFc (**1**) have been acquired at 123, 173, 232, and 298 K and the rmsav data calculated from the corresponding anisotropic displacement parameters  $U_{ij}$  are compared to detailed ME spectroscopic results over the range  $88 < T < 385$  K. In addition, lattice dynamical parameters have been extracted from ME data for  $\text{DMFc}^+\text{BF}_4^-$  (**2**), the co-crystalline solid-state adduct (intercalate) of  $\text{C}_{60}$  and DMFc reported by Stanghellini et al.<sup>[8]</sup> (**3**), and the mononuclear bucky ferrocene  $\text{CpFe}(\text{CH}_3)_5\text{C}_{60}$  reported by Nakamura and Matsuo et al.<sup>[9]</sup> (**4**). The details of the rmsav data for the metal atom in these structurally related complexes are described in detail in the present study.

## Results and Discussion

A representative ME spectrum of **1** at 298 K is shown in Figure 1. It consists of a single quadrupole doublet with a line width (*fwhm*) of  $0.243 \pm 0.005$   $\text{mm s}^{-1}$  at room temperature. The resonance effect under these conditions is about 2.8%, and the data were treated with the “thin absorber” approximation. The hyperfine parameters [isomer shift (IS) and quadrupole splitting (QS)] for **1** have been reported earlier.<sup>[10]</sup> The area ratio of the two components of the doublet spectrum are essentially temperature independent over the range  $90 < T < 370$  K, thus indicating no appreciable anisotropy in the metal atom motion parallel and perpendicular

[a] Racah Institute of Physics, Hebrew University of Jerusalem, 91904 Jerusalem, Israel  
E-mail: Herber@vms.huji.ac.il

[b] Institut für Mineralogie/Petrographie, Universität Innsbruck, Innrain 52, 6020, Innsbruck, Austria

[c] Institut für Anorganische Chemie, Universität Innsbruck, Innrain 52a, 6020, Innsbruck, Austria

lar to the symmetry axis passing through the two five-membered rings and the Fe atom. This is in contrast to the observations made in the case of the parent ferrocene,<sup>[3,4]</sup> in which this anisotropy is significant over a similar temperature range.

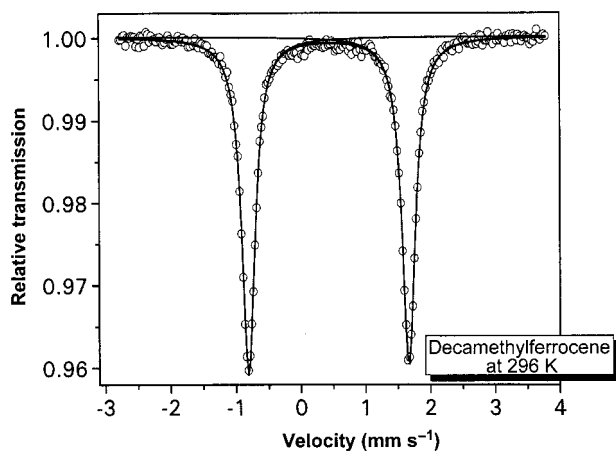


Figure 1.  $^{57}\text{Fe}$  Mössbauer spectrum of decamethylferrocene (**1**) at room temperature. The velocity scale is with respect to the centroid of an  $\alpha\text{-Fe}$  absorber spectrum at room temperature.

The recoil-free fraction scales with the area ( $A$ ) under the resonance curve in the “thin absorber” approximation; that is  $\ln[A(T)/A(r)]$  [where  $A(T)$  is the area under the resonance curve at temperature  $T$ , and  $A(r)$  is a reference temperature] scales with  $\ln f$ . The recoil-free fraction,  $f$ , in turn, is given by

$$f = \exp(-k^2 \langle x_{\text{ave}}^2 \rangle)$$

where  $k$  is the wave vector of the ME gamma ray ( $7.3039 \text{ \AA}^{-1}$ ) and  $\langle x_{\text{ave}}^2 \rangle$  is the mean square amplitude of the metal atom motion. It follows that an estimate of the msav can be extracted from the temperature-dependent spectral area values extracted from the ME data. The temperature dependence of the logarithm of the area under the resonance curve is summarized graphically in Figure 2. It is immediately obvious from these data that there is significant curvature in this dependence, especially at higher temperatures (i.e. above about 300 K), in contrast to what is usually observed in organometallic solids. Moreover, the highest temperature at which reliable ME data can be acquired is approximately 385 K, which is some 165 K below the melting point of this compound. It may be postulated that the onset of ring rotation at higher temperatures, which increases the metal–ring distances, increases the rmsav of the iron atom to the point where the ME is no longer observable. However, this assumption has been questioned on the basis of a density of states (DOS) study at 25 K, carried out at ESRF by Chumakov and van Buerck.<sup>[11]</sup> This study showed that the DOS is almost completely defined by the data within the first 9 meV and that at higher temperatures (above 100 K) all these modes are effectively populated. However, their DOS data do not directly elucidate the reason for the non-linearity referred to above except to indicate that an additional effect sets in at higher temperatures.

Moreover, the X-ray data in the range  $123 \leq T \leq 298 \text{ K}$  show that the distance from the metal atom to the centers of the five-membered rings increases by only 0.45% with increasing temperature. Extrapolation of the linear low-temperature dependence of  $-\ln[A(T)]$  to 298 K shows that this extrapolation gives a value some 10% smaller than what is observed experimentally. Thus, the decrease in  $f$  is not well accounted for by the onset of ring-rotation, and this dynamic may not be solely responsible for the non-linearity in the  $\ln A(T)$  vs.  $T$  data summarized in the figure. A “softening” of the lattice (as probed by the Fe ion) well below  $T_{\text{mp}}$  must be accounted for by another mechanism. Differential scanning calorimetry data by Kobayashi et al.<sup>[12]</sup> have shown the existence of two solid phase transitions at  $397 \pm 1$  and  $501 \pm 2 \text{ K}$  involving uniaxial reorientation of the whole molecule about its  $C_5$  axis. NMR spectroscopic data by Waugh et al.<sup>[13]</sup> and Pines et al.<sup>[14]</sup> have been interpreted in terms of a  $2\pi/5$  jump process involving an energy barrier of about 143 and 140 meV, respectively, but these processes would not be significant in the solid in the low-temperature regime. The barrier to internal rotation for the gas-phase molecule has been reported<sup>[7b]</sup> to be 43.4 meV.

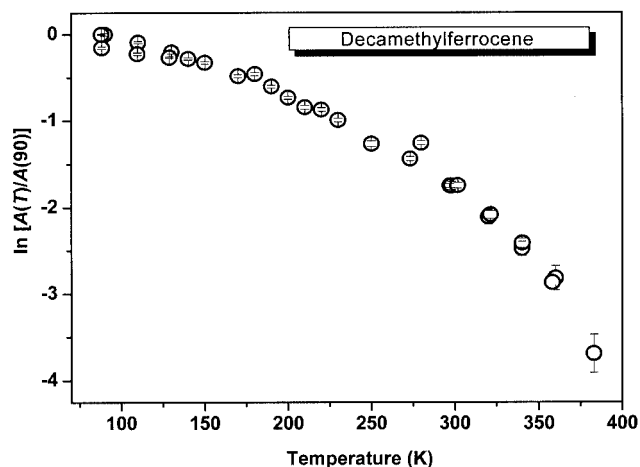


Figure 2. Temperature dependence of  $\ln[A(T)/A(90)]$  for **1**. The low-temperature data were obtained with a natural abundance  $^{57}\text{Fe}$  sample and were fitted using the optically “thin” absorber approximation. The high-temperature data were acquired using an enriched  $^{57}\text{Fe}$  sample as discussed in the text.

The  $\ln[A(T)]$  data have been scaled so that the low-temperature regime passes through (0,0) at  $T = 0 \text{ K}$ . The resulting curve can be well fitted by a second-order polynomial function from which  $\ln A$ , and hence the msav of the metal atom, can be calculated at all temperatures. These values, in turn, can be compared to those extracted from the anisotropic displacement parameters of the single-crystal X-ray diffraction experiment, and are shown in Figure 3 by the filled data points. The agreement between these two sets of values, at least up to 298 K, appears to be quite satisfactory, and validates the interpretation of the Mössbauer data in terms of  $\langle x_{\text{ave}}^2 \rangle$ . A similar comparison for ferrocene, based on the data of Brock and Fu,<sup>[15]</sup> has been reported earlier.<sup>[3]</sup>

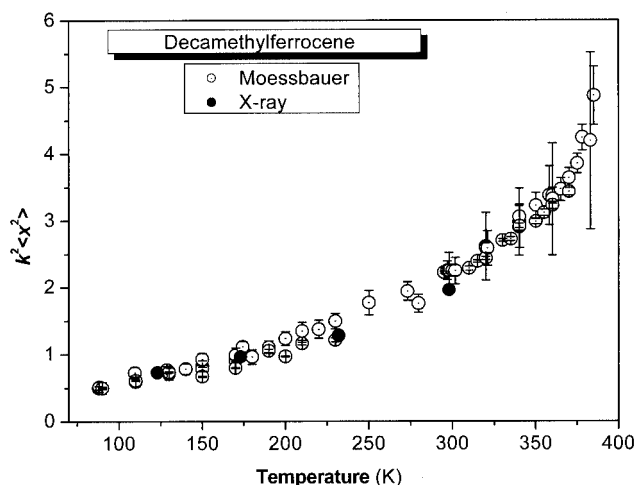


Figure 3. Temperature-dependence of the  $k^2\langle x_{\text{ave}}^2 \rangle$  values for **1** extracted from the ME data (open circles) and from the single-crystal X-ray diffraction data (filled circles). The average errors in the X-ray values are  $\pm 0.00064$ ,  $\pm 0.00112$ ,  $\pm 0.0014$ , and  $\pm 0.00138 \text{ \AA}^2$  at 298, 223, 173, and 123 K, respectively.

A summary of the rmsav of the metal atom in **1** at five different temperatures calculated from the X-ray data and the ME experiments is given in Table 1, which includes the comparable data for related systems to be discussed below. Thus, despite the uncertainty concerning the origin of the non-linearity in the  $\ln f$  vs.  $T$  data shown in Figure 2, it is clear that the ME data can be used to estimate the rmsav of the metal atom in such organometallic solids.

Table 1. Root-mean-square amplitudes-of-vibration (rmsav;  $\text{\AA}$ ) of the iron atom in a number of structurally related organometallics discussed in the text.

Ferrocene	<b>4</b>	<b>3</b>	<b>2</b>	DMFc (ME)	DMFc (X-ray)	Temp. [K]
0.131	0.102	0.115	0.105	0.107	0.104	100
0.154	0.120	0.140	0.126	0.122	0.125	150
0.183	0.137	0.157	0.145	0.143	0.143	200
0.202	0.156	0.182	0.162	0.182	0.165	250
0.222	0.174	0.202	0.177	0.205	0.191	300

A molecular system closely related to the neutral species **1** is that obtained by one-electron oxidation of **1**, in which the cationic charge is balanced by the presence of either  $\text{BF}_4^-$  or  $\text{PF}_6^-$  anions. The ME spectra of the former compound, **2**, consist of a single broad resonance line which arises from spin-lattice relaxation of the paramagnetic metal site. The ME hyperfine parameters of **2** are listed in Table 2, and are similar to those of the corresponding  $\text{BF}_4^-$

salt. It is, however, interesting to note that the  $\ln[A(T)/A(90)]$  vs.  $T$  data are well fitted by a linear regression over the temperature range  $90 \leq T \leq 360 \text{ K}$ , in contrast to the data for **1** discussed above. The  $\ln A(T)$  data for **2** are shown graphically in Figure 4 (filled data points) together with those for **3** and **4** (to be discussed below). The rmsav data for **2** listed in Table 1 are very similar to those reported for **1** at a given temperature, except at 300 K, which is indicative of a similarity in the Fe–ligand interaction, especially in the lower temperature regime. Unfortunately, the relevant iron atom  $U_{ij}$  data are not available in the literature, so no direct comparison with X-ray data for the cationic complex **2** can be effected at the present time.

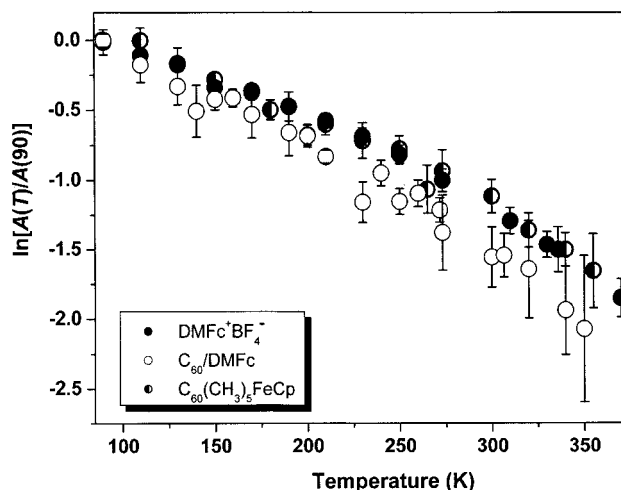


Figure 4. Temperature-dependence of the  $\ln(A)$  data (normalized to the 90 K value) for **2**, **3**, and **4**.

The data in Table 1 includes rmsav results obtained from ME experiments on the co-crystalline product  $\text{C}_{60}\cdot\text{DMFc}$  (**3**) reported by Stanghellini et al.,<sup>[8]</sup> which is similar to the  $\text{C}_{60}$  ferrocene intercalate reported by Crane et al.<sup>[16]</sup> for which the ME characterization has been reported from this laboratory.<sup>[17]</sup> The ME hyperfine parameters of **3** are included in Table 2. The  $U_{ij}$  values for the iron atom in **3** have been determined at 150 K by Stanghellini et al.<sup>[8]</sup> and the calculated  $k^2\langle x_{\text{ave}}^2 \rangle$  value of 1.10 is in good agreement with the ME extracted value of 1.02 at the same temperature. The remainder of the rmsav data for **3** listed in Table 1 are those derived from the ME data as described for **1** above. It is noted from these data that the rmsav of the metal atom in **3** is comparable to that in **1** at the same temperature, suggesting that this parameter reflects *intra*- rather than *intermolecular* forces. It is also worth noting

Table 2. Mössbauer effect (ME) hyperfine parameters at 90 K and related values for the compounds discussed in the text. The parenthetical number(s) are the errors associated with the last figure(s) for each entry.

	IS(90) [mm s <sup>-1</sup> ]	QS(90) [mm s <sup>-1</sup> ]	$-\text{d}(\text{IS})/\text{d}T$ [10 <sup>-4</sup> mm s <sup>-1</sup> K <sup>-1</sup> ]	$-\text{d}(\ln A)/\text{d}T$ [10 <sup>-3</sup> K <sup>-1</sup> ]	$M_{\text{eff}}$ [Daltons]	$\Theta_{\text{M}}$ [K]
<b>1</b>	0.492(3)	2.473(2)	3.17(13)	(curv.)	131(3)	n.a.
<b>2</b>	0.460(5)	0.189(5)	3.82(8)	5.93(4)	109(5)	110(5)
<b>3</b>	0.501(5)	2.451(5)	2.32(4)	6.82(7)	85(3)	116(5)
<b>4</b>	0.575(4)	2.475(4)	5.36(5)	7.42(17)	78(2)	116(5)

that the temperature dependence of the  $\ln[A(T)/A(90)]$  data for **3** over the temperature range  $89 \leq T \leq 350$  K are well accounted for by a linear regression ( $cc = 0.994$  for 23 data points) so that the lattice “softening” observed in **1** is again absent in **3**. Since both the isomer shift and the recoil-free fraction data show a linear temperature-dependence over the total temperature range, it is possible to calculate<sup>[18]</sup> both an “effective vibrating mass” ( $M_{\text{eff}}$ ) and a “Mössbauer lattice temperature” ( $\Theta_M$ ) of  $85 \pm 3$  D and  $116 \pm 5$  K, respectively. Clearly, these data refer to the high-temperature limiting values, i.e.  $T_{\text{exp}} > \Theta_M/2$ . The difference between the calculated  $M_{\text{eff}}$  (85 D) and the “bare” atom mass (57 D) reflects the covalency of the metal atom–ligand interaction, as discussed earlier.<sup>[19]</sup> The  $[k^2 \langle x^2 \rangle]^{1/2}$  values at five different temperatures, calculated from the  $\ln A(T)$  data as noted above, and making the assumption that the high-temperature limiting slopes extrapolate to  $f = 0$  as  $T \rightarrow 0$ , are summarized graphically in Figure 5.

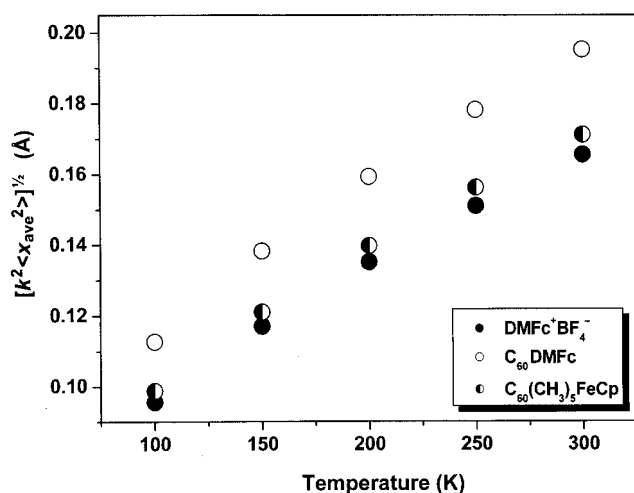


Figure 5. The  $[k^2 \langle x^2 \rangle]^{1/2}$  parameters for **2**, **3**, and **4** at five different temperatures calculated from the high temperature ( $T > \Theta_M/2$ ) slopes of the data shown in Figure 4, as discussed in the text.

Finally, a related organometallic structure in which the iron atom is ligated to two five-membered rings and in which there are five methyl groups on the  $\text{C}_{60}$  sphere, in near proximity to the metal center, is provided by the “bucky ferrocene” compound **4**, for which the details of the ME parameters have been reported earlier.<sup>[4]</sup> In this molecule the iron atom “sees” an unsubstituted Cp ring in one direction and a similar Cp ring in the opposite direction, with, however, five methyl groups attached to the next neighbor carbon atoms of the  $\text{C}_{60}$  sphere. The ME hyperfine parameters and derived data are included in Table 1 and the rmsav values for the iron atom are listed in Table 2 and included in Figure 5. As in the case of **2** and **3**, the  $\ln f$  vs.  $T$  plot is linear over the temperature range  $210 \leq T \leq 370$  K as already noted.<sup>[1]</sup> As indicated in Figure 5, the rmsav of the metal atom in **4** is very nearly identical to that in **1** and **3**. Presumably the massive fullerene moiety ligated to the Fe center plays no critical role in the magnitude of the rmsav of the metal atom in these complexes.

## Summary and Conclusions

An improved efficient synthesis of  $^{57}\text{Fe}$ -labeled decamethylferrocene ( $^{57}\text{Fe}$  DMFc) has been developed. The resulting product has been characterized by elemental and isotopic composition, single-crystal X-ray diffraction, and IR and NMR spectroscopic data. The availability of  $^{57}\text{Fe}$  DMFc, in turn, has made it possible to use temperature-dependent Mössbauer effect spectroscopy to elucidate the hyperfine interactions in this material at high temperatures, as well as the temperature-dependence of the recoil-free fraction of the metal atom. From these data it is possible to determine the mean-square-amplitude-of-vibration of the iron atom motion, and to compare these results with those extracted from single-crystal X-ray diffraction data. The agreement between these two data sets in the temperature range 80 to 300 K is quite satisfactory within the quoted experimental errors. The origin of the non-linearity observed in the recoil-free fraction data, as well as the vanishingly small value of this parameter at temperatures about 165 K below the melting point of DMFc is assumed to be due in part to the onset of ring rotation in the solid, but may have an additional contribution not well elucidated by the presently available data. The comparison of the Fe vibrational amplitude as a function of temperature for a number of structurally related ferrocene-type systems should lead to a clearer understanding of the relationship between the microscopic architecture and the dynamic behavior of the metal atom in these structures.

## Experimental Section

A commercial sample of **1** was recrystallized from trichloroethylene and used without further purification for the ME studies. A sample of  $^{57}\text{Fe}$ -enriched **1** was prepared as described below and used for acquiring data in the high-temperature regime ( $T \geq 300$  K) where the recoil-free fraction values ( $f$ ), which determine the area under the resonance curve, become so small that natural abundance samples would require inordinately long data acquisition times. Single crystal samples of **1** for the X-ray diffraction studies were grown as described below. A sample of **2** was prepared in the Innsbruck laboratory and used for Mössbauer studies as received. Complex **3** was similarly made available by Profs. Stanghellini and Viterbo and used as received. A sample of **4** was provided by Profs. Nakamura and Matsuo, and again used as received.

Temperature-dependent ME studies were carried out as described previously<sup>[1–5]</sup> and spectrometer calibration was effected using a  $10.52 \text{ mg cm}^{-2}$   $\alpha\text{-Fe}$  foil at room temperature, which also served as the isomer-shift reference point. Temperature control was monitored using the DASWIN program of Glaberson and Brettschneider,<sup>[20]</sup> and confirmed that the indicated temperatures were constant to better than  $\pm 0.2$  K over the data acquisition periods (typically 8–24 hours) at each temperature.

For the structural investigations of **1**, a rhomb-shaped crystal of good optical quality ( $0.14 \times 0.14 \times 0.16 \text{ mm}^3$  in size) was selected and mounted on a glass fiber. Data collections at four different temperatures were performed using graphite-monochromated  $\text{Mo-K}\alpha$  radiation on a Stoe IPDS-II diffractometer equipped with a 700 Series Oxford Cryostream nitrogen gas stream cooler. The mor-



phology of the crystals was described by external faces and an analytical absorption correction based on the indexed faces was applied. Further data reduction included Lorentz and polarization corrections. The subsequent least-squares refinements were accomplished with the program SHELX97.<sup>[21]</sup> The corresponding X-ray data for **3** have been reported in the literature.<sup>[8]</sup>

### Synthesis and Characterization of [<sup>57</sup>Fe]Decamethylferrocene

**Instrumentation:** Microwave reactor: Synthos 3000, Anton Paar GmbH, Austria; Kugelrohr apparatus: Buechi GKR-51, Switzerland. IR spectra were measured with a Nicolet 5700 FT-IR with an ATR diamond window, and <sup>1</sup>H and <sup>13</sup>C NMR spectra were recorded in CDCl<sub>3</sub> solution with a Bruker Avance DPX 300 spectrometer. All organometallic reactions were carried out under an inert atmosphere using standard Schlenk techniques. Solvents were distilled, dried, and deoxygenated prior to use. Starting compounds not specifically referred to are commercially available by several suppliers. Purchased chemicals were used without any further purification.

<sup>57</sup>Fe-enriched iron powder (95%) was purchased from ATM, Advanced Materials Technologies. From this starting material, enriched <sup>57</sup>FeCl<sub>2</sub> was prepared by oxidation with methanolic hydrogen chloride in a microwave reactor by the novel procedure described below. This synthesis is also a low-temperature preparation in solution,<sup>[22]</sup> but avoids the concomitant formation of chlorobutanol from HCl and THF, which is difficult to separate from methylated ferrocenes during workup. The <sup>57</sup>Fe-labeled decamethylferrocene was then prepared from <sup>57</sup>FeCl<sub>2</sub> by complexation with the [CpMe<sub>5</sub>]<sup>−</sup> anion in analogy to the synthesis of [<sup>57</sup>Fe]octamethylferrocene.<sup>[23]</sup> In contrast to octamethylferrocene, decamethylferrocene is very easily oxidized on silica and alumina-packed chromatography columns, which results in extremely reduced yields if any chromatographic purification is required. The elemental and isotopic composition of [<sup>57</sup>Fe]decamethylferrocene was determined by means of HR mass spectrometry (Finnigan MAT 95). The exact monoisotopic molecular weight was measured using the following HR-FAB-MS conditions: Cs gun: 20 kV, 2 μA; glycerol matrix, resolution *R* = 8000, E-scan, average over 20 scans. The determination of the <sup>57</sup>Fe/<sup>56</sup>Fe isotope ratio of the target compound gave a <sup>57</sup>Fe content of >95.0%.

**Synthesis of Anhydrous <sup>57</sup>FeCl<sub>2</sub>:** <sup>57</sup>Fe powder (35 mg, 0.62 mmol) was fixed on a magnetic stirring bar and placed in a Teflon-lined microwave reactor along with 6 mL of a 1.25 M solution of hydrochloric acid in methanol (6 mL required to immerse the internal temperature probe), whereupon a slight evolution of hydrogen was observable. The reaction mixture was heated to 150 °C within 1 min and held at this temperature for 50 min. Afterwards, it was cooled by the fan-device for 20 min. The liner was opened under a stream of nitrogen and the contents transferred to a Schlenk tube. The <sup>57</sup>Fe powder was completely dissolved, although the yellowish coloration indicated the presence of iron(III) salts. Subsequently, the solvent and excess hydrogen chloride were stripped off on a vacuum line (oil pump) whilst heating to 40 °C in a water bath, and the crude iron chlorides triturated for 5 min with chlorotrimethylsilane (1 mL) in order to remove protic solvent residuals. The chlorotrimethylsilane was then pumped off whilst shaking the Schlenk tube in such a way that the crude iron chloride was deposited in a layer covering the lower part of the tube. Afterwards, the remainder was rinsed with hexamethyldisilane (1 mL) and evacuated again to yield an off-white material. Anhydrous THF (40 mL) was added to the Schlenk tube and the solution was stirred magnetically with an additional 5 mg of excess <sup>57</sup>Fe powder adhered to the stirring bar to give a clear white solution of FeCl<sub>2</sub> within 2 min. The THF

solution was cooled to −40 °C under nitrogen and used for the complexation step below.

**Synthesis of [<sup>57</sup>Fe]Decamethylferrocene:** Anhydrous THF (60 mL) was placed in a second Schlenk tube and 1,2,3,4,5-pentamethyl-1,3-cyclopentadiene (0.95 mL, 170 mg, 1.26 mmol; Chem. Abstr. registry no. 4045-44-7) was added from a syringe. The solution was cooled to −40 °C under nitrogen and butyllithium (0.80 mL, 1.6 M in hexane) was added to give a yellowish cloudy suspension. After 30 min the external cooling bath was removed and the reaction mixture was warmed to 10 °C whilst stirring. Afterwards, the reaction mixture was again recooled to about −30 °C. The <sup>57</sup>FeCl<sub>2</sub>/THF solution obtained by the procedure described above was added with a cannula and the stirring bar holding the excess elemental iron powder was also transferred. The resulting reaction mixture gradually turned black. After 90 min, the cooling bath was removed and the reaction mixture was ultrasonicated for 30 min. The solvents were removed on the vacuum line and the remainder was partitioned between diethyl ether (30 mL) and water (40 mL) in a separating funnel. The aqueous layer was washed with diethyl ether (30 mL) and the combined organic phases again extracted with water (2 × 30 mL). The organic phase was dried with anhydrous sodium sulfate and filtered. Evaporation (rotary evaporator) and drying (oil pump) yielded 105 mg of crude decamethylferrocene as a yellow-orange powder (52% of theoretical yield based on <sup>57</sup>Fe). Finally, the crude product was sublimed<sup>[24]</sup> in a Kugelrohr apparatus at 200 °C on a vacuum line. HR-MS calcd. for C<sub>20</sub>H<sub>30</sub><sup>57</sup>Fe<sub>1</sub> (DMFc): 327.1696; found 327.1705 (cation; rel. intensity 27.4); calcd. for C<sub>19</sub><sup>13</sup>CH<sub>30</sub><sup>57</sup>Fe<sub>1</sub> (DMFc): 328.1730; found 328.1699 (cation; rel. intensity 6.2). IR data (ATR):  $\tilde{\nu}$  = 2962.5 cm<sup>−1</sup> s, 2943.2 m, 2891.5 s, 2851.7 m, 2712.0 w, 1473.4 m, 1448.0 m, 1424.2 m, 1371.9 s, 1353.0 w, 1259.3 m, 1068.8 s, 1024.6 vs, 867.5 w, 796.5 s, 698.7 ws, 589.4 w, 536.1 w, 507.2 w, 449.4 vs, 416.6 m. <sup>1</sup>H NMR (CDCl<sub>3</sub>):  $\delta$  = 1.67 ppm (s, methyl-*H*). <sup>13</sup>C NMR (CDCl<sub>3</sub>):  $\delta$  = 9.59, (methyl-*C*, <sup>1</sup>J<sub>C,H</sub> = 125.4 Hz), 79.70 ppm (Cp-*C*). DMFc is only sparingly soluble in methanol; alternatively, suspending the crude material by ultrasonication then centrifuging the mixture allows removal of any organic impurities. Crystals suitable for X-ray structure determinations were grown by slow evaporation of the solvent from a solution in 2-methylbutane at ambient temperature. In order to recover any residual unreacted <sup>57</sup>Fe material, the aqueous extracts containing precipitated iron(III) hydroxide (formed by oxidation with ambient oxygen during workup) were centrifuged. Iron(III) chloride may be reconverted to iron(II) chloride by dissolving the separated Fe(OH)<sub>3</sub> in methanolic hydrogen chloride and drying/reducing with trimethylchlorosilane/hexamethyldisilane as described above.

### Acknowledgments

The authors are indebted to Prof. H. Schottenberger both for the single crystals of **1** used in the acquisition of the X-ray data and also for providing the <sup>57</sup>Fe-labeled samples used in the ME experiments. Similarly, we are grateful to Profs. Nakamura and Matsuo for providing a sample of **4** for study, and Profs. P. L. Stanghellini and D. Viterbo not only for providing the sample of **3** for the ME experiments but also for sharing the results of their X-ray investigation with us.

- [1] R. H. Herber, I. Nowik, Y. Matsuo, M. Toganoh, Y. Kuninobu, E. Nakamura, *Inorg. Chem.* **2005**, *44*, 5629–5635.
- [2] I. Nowik, M. Wagner, R. H. Herber, *J. Organomet. Chem.* **2003**, *688*, 11–14.

- [3] R. H. Herber, I. Nowik, *Hyperfine Interact.* **2002**, *144*, 249–253.
- [4] R. H. Herber, I. Nowik, *Hyperfine Interact.* **2001**, *136*, 699–703.
- [5] R. H. Herber, I. Nowik, *Solid State Sci.* **2002**, *4*, 691–694 and references cited therein.
- [6] Yu. T. Struchkov, V. G. Andrianov, T. N. Sal'nikova, I. R. Lyat'ifov, R. B. Materikove, *J. Organomet. Chem.* **1978**, *145*, 213–223.
- [7] a) D. P. Freyberg, J. L. Robbins, K. N. Raymond, J. C. Smart, *J. Am. Chem. Soc.* **1979**, *101*, 892–897; b) A. Almenningen, A. Haaland, S. Samdal, J. C. Smart, *J. Organomet. Chem.* **1979**, *173*, 293–299.
- [8] A. Arrais, E. Diana, R. Gobetta, M. Milanesio, D. Viterbo, P. L. Stanghellini, *Eur. J. Inorg. Chem.* **2003**, 1186–1192.
- [9] M. Sawamura, Y. Kuninobu, M. Toganoh, Y. Matsuo, Y. Yamataka, E. Nakamura, *J. Am. Chem. Soc.* **2002**, *124*, 9354–9355; Y. Matsuo, Y. Kuninobu, S. Ito, E. Nakamura, *Chem. Lett.* **2004**, 33 and references cited therein.
- [10] R. H. Herber, in *Unusual Structures and Physical Properties in Organometallic Chemistry* (Eds. M. Gielen, R. Willem, B. Wrackmeyer), John Wiley & Sons, Chichester, UK, **2002**, pp. 210–211.
- [11] A. Chumakov, U. van Buerke, private communication.
- [12] T. Kobayashi, H. Ohki, R. Ikeda, *Mol. Cryst. Liq. Cryst. Sci. Technol., Sect. A* **1994**, *257*, 279.
- [13] D. Suwelak, W. P. Rothwell, J. S. Waugh, *J. Chem. Phys.* **1980**, *73*, 2559–2569.
- [14] D. E. Wemmer, D. J. Ruben, A. Pines, *J. Am. Chem. Soc.* **1981**, *103*, 28–33.
- [15] C. P. Brock, Y. Fu, *Acta Crystallogr. Sect. B* **1997**, *53*, 928 (model R1ZH).
- [16] J. D. Crane, P. B. Hitchcock, H. W. Kroto, R. Taylor, D. R. M. Walton, *J. Chem. Soc., Chem. Commun.* **1992**, 1764.
- [17] P. P. R. Birkett, K. Kordatos, J. D. Crane, R. H. Herber, *J. Phys. Chem. B* **1997**, *101*, 8975–8978.
- [18] R. H. Herber, in *Chemical Mossbauer Spectroscopy* (Ed.: R. H. Herber), Plenum Press, New York, **1984**, pp. 199–121.
- [19] R. H. Herber, I. Nowik, D. A. Loginov, Z. A. Starikova, A. R. Kudinov, *Eur. J. Inorg. Chem.* **2004**, 3476–3483 and references cited therein.
- [20] W. Glaberson, M. Brettschneider, see: [www.phys.huji.ac.il/~glabersn](http://www.phys.huji.ac.il/~glabersn).
- [21] G. M. Sheldrick, *SHELX97 Program for Crystal Structure Analysis* (release 97-2), University of Göttingen, Germany, **1998**.
- [22] M. Aresta, C. F. Nobile, D. Petruzzelli, *Inorg. Chem.* **1977**, *16*, 1817.
- [23] R. H. Herber, I. Nowik, H. Schottenberger, K. Wurst, N. Schuler, A. G. Mueller, *J. Organomet. Chem.* **2003**, *682*, 163; B. S. Özman, *Chem.-Ztg.* **1976**, *100*, 143.
- [24] T. Kiyobayashi, M. E. Minas da Piedade, *J. Chem. Thermodyn.* **2001**, *33*, 11.

Received: March 12, 2006  
Published Online: June 28, 2006